Supplemental Information

Supplemental Figures

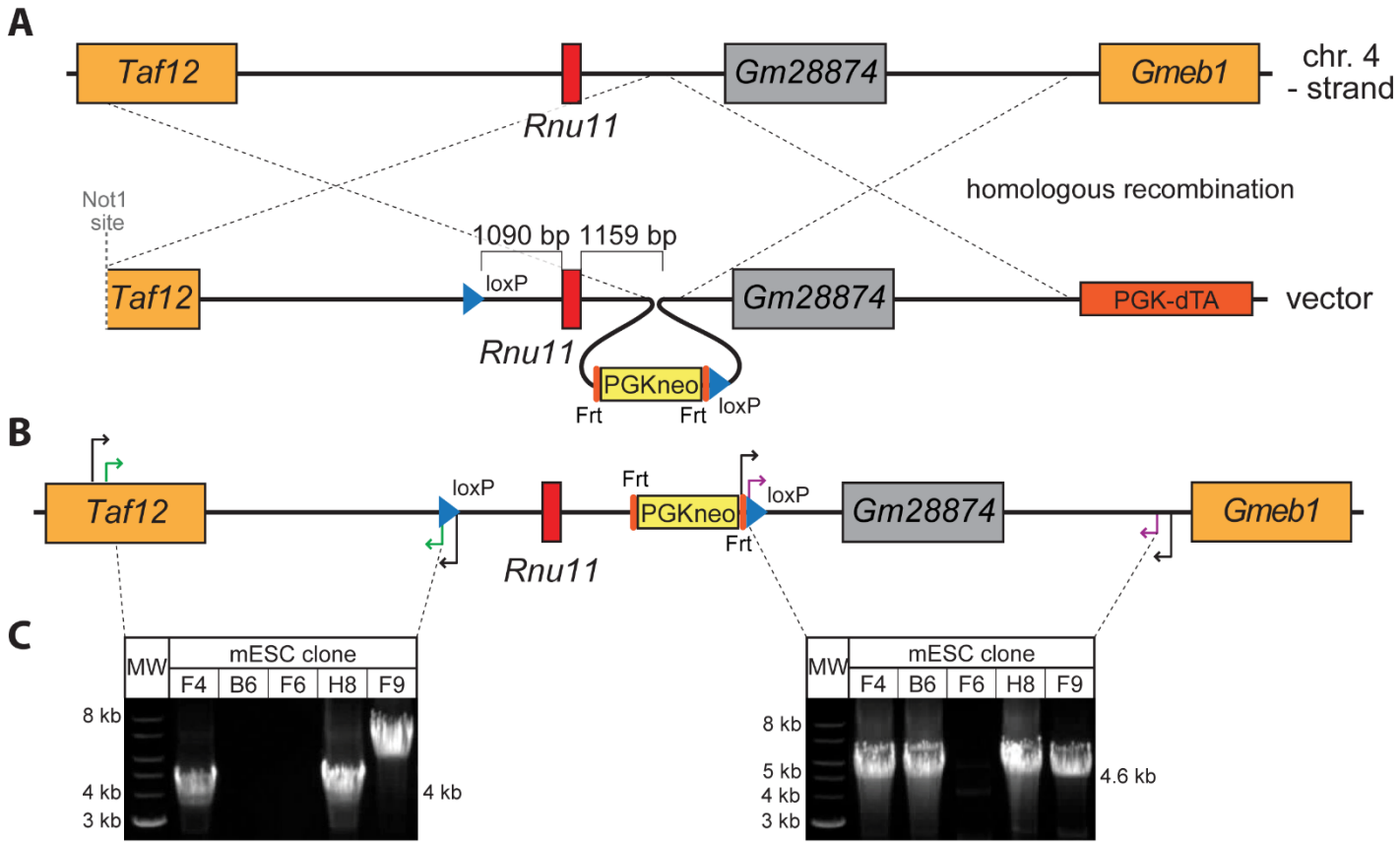

Figure S1. Generation and confirmation of the *Rnu11* cKO mice. Related to Figure 1. (**A**) Schematic of the *Rnu11* locus. The gray box represents the predicted gene *Gm28874*. Below the *Rnu11* locus schematic is the targeting construct used to introduce the loxP sites by homologous recombination (dashed lines). (**B**) Schematic representing the targeted allele, showing the primers used to interrogate the 5' loxP site (black and green arrows, left) and the 3' loxP site (black and purple arrows, right). For the 5' loxP site primer set, the outermost forward primer (black arrow, left) was designed outside the 5' arm of homology, with the outermost reverse primer (black arrow, left) positioned downstream of the 5' loxP site. The inner set of nested primers (green arrows) were designed in the 5' arm of homology and within the 5' loxP site, respectively. For the 3' loxP site primer set, the outermost forward primer (black arrow, right) was designed in the Frt site located upstream of the 3' loxP site, with the outermost reverse primer (black arrow, right) positioned downstream of the 3' arm of homology. The inner set of nested primers (purple arrows) were designed in the 3' loxP site and the 3' arm of homology, respectively. (**C**) Agarose gel images of long-range nested PCRs, performed on genomic DNA (gDNA) from targeted ES cells, using the 5' loxP site primer set (black and green arrows, left) and the 3' loxP site primer set (black and purple arrows, right). The number at the right of each gel image represents the expected product size produced from this strategy.

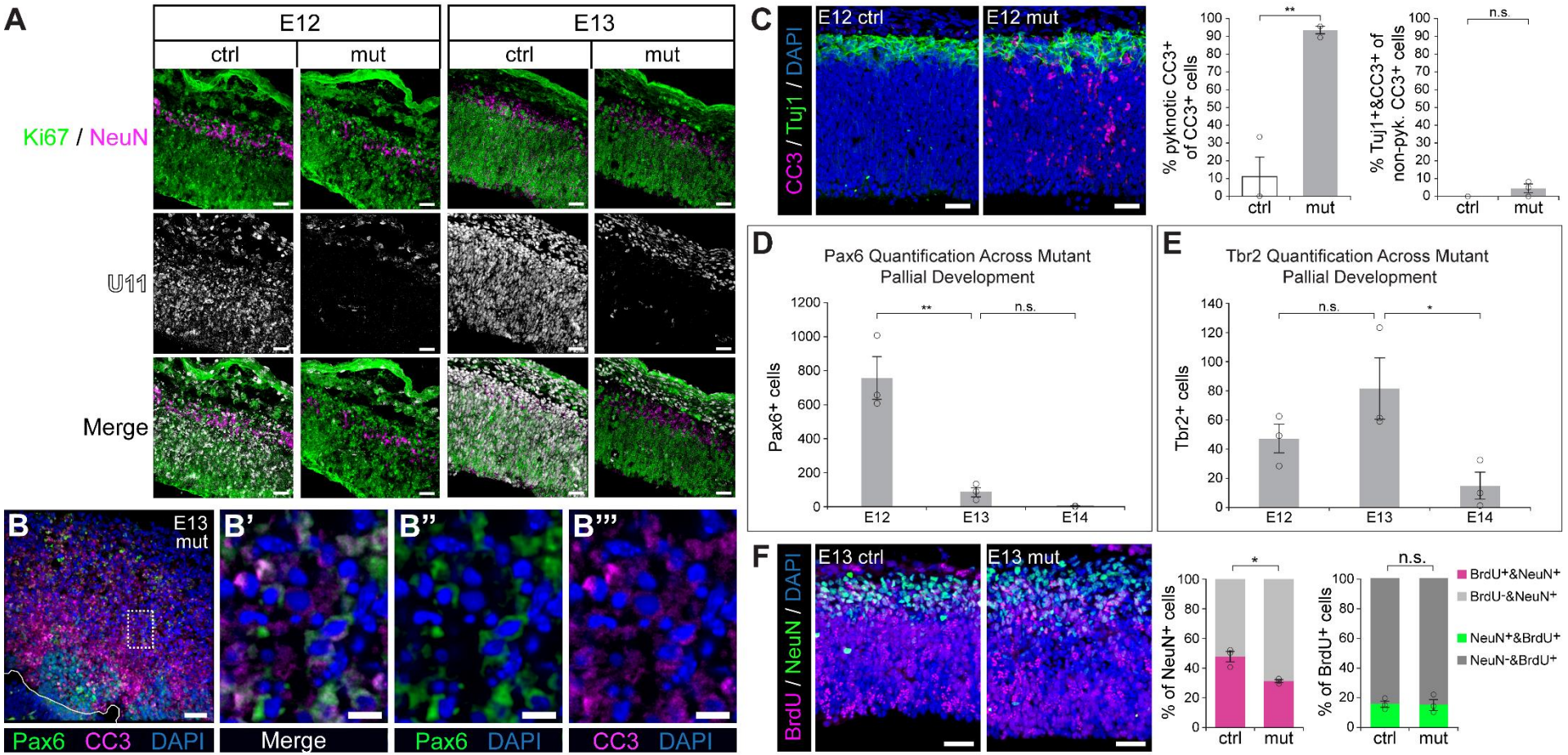

Figure S2. U11 loss and death of self-amplifying RGCs in the mutant pallium. Related to Figure 3. (**A**) Separated channels for sagittal section U11 FISH (middle row) and immunofluorescence (IF) for Ki67 (green) and NeuN (magenta) (top row), with overlay (bottom row), from the E12 and E13 control (ctrl) and mutant (mut) pallium. Scale bars=30 µm. (**B**) IF for Pax6 (green) and cleaved caspase 3 (CC3, magenta) on sagittal section of E13 mutant pallium. White line marks the boundary between the subpallium and the pallium. Scale bar=30 µm. (**B'-B'''**) Magnified images of the dashed box in (**B**), showing overlay of all channels (**B'**), Pax6 and DAPI (**B''**), and CC3 and DAPI (**B'''**). Scale bars=7 µm. (**C**) IF for CC3 (magenta) and Tuj1 (green) in sagittal section of the E12 ctrl and mut pallium, with bar graphs showing the percentage of $CC3^+$ cells that were pyknotic (left) and the percentage of non-pyknotic $CC3^+$ cells that were $Tuj1^+$ (right). Scale bars=30 µm. (**D-E**) Bar graphs showing quantification of cells with nuclear Pax6 staining (**D**) or cells with nuclear Tbr2 staining (**E**) across development in the mutant pallium, from E12 and E14. Statistical significance across the three tested time-points was determined by one-way ANOVA, followed by Tukey's multiple comparison test to determine specific *P* values. (**F**) IF for BrdU (magenta) and NeuN (green) in the E13 ctrl and mut pallium, which had been pulsed with BrdU at E12. Scale bars=30 µm. At right are bar graphs showing the percentage of $NeuN^+$ cells that were $BrdU^+$ in the E13 pallium, or the percentage of non-pyknotic $BrdU^+$ cells that were $NeuN^+$ in the E13 pallium. Statistical significance was determined by two-tailed student's *t*-tests (Table S8). Quantification data are represented as mean±SEM from *N*=3 for each condition per time-point; individual data points are superimposed on bar graphs. Non-pyk.=non-pyknotic. n.s.=not significant; *=*P*<0.05; **=*P*<0.01.

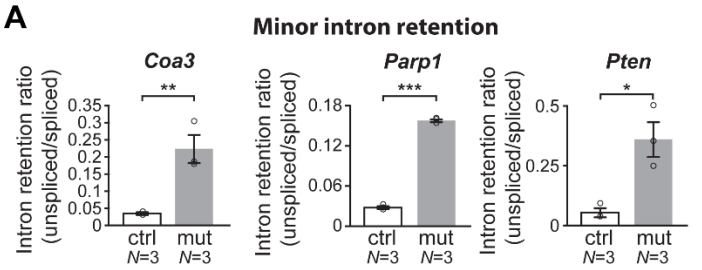

B **DAVID analysis of MIGs with elevated minor intron retention**

GO-term Functional Enrichment	Genes	Benjamini
nucleoplasm	41	9.405E-6
nucleotide binding	36	9.190E-4
protein transport	19	3.069E-3
cell cycle	18	9.714E-3
nuclear pore complex assembly	4	2.007E-2
poly(A) RNA binding	22	2.176E-2
centrosome	13	2.324E-2

Figure S3. Validation of expression and minor intron retention changes in the E12 mutant pallium. Related to Figure 5. (**A**) Minor intron retention of *Coa3* (left), *Parp1* (middle), and *Pten* (right) in the E12 ctrl and mut pallium, as determined by qRT-PCR. The value plotted is the average ratio of normalized unspliced expression/normalized spliced expression ± SEM from *N*=3 for each condition. Individual data points are superimposed on the bar graphs. Statistical significance was determined by two-tailed student's *t*-tests (Table S8). *=*P*<0.05, **=*P*<0.01, ***=*P*<0.001. (**B**) GO Terms enriched for by DAVID analysis of MIGs with statistically significant elevated minor intron retention in the E12 mutant pallium, with cell cycle-related terms highlighted in yellow.

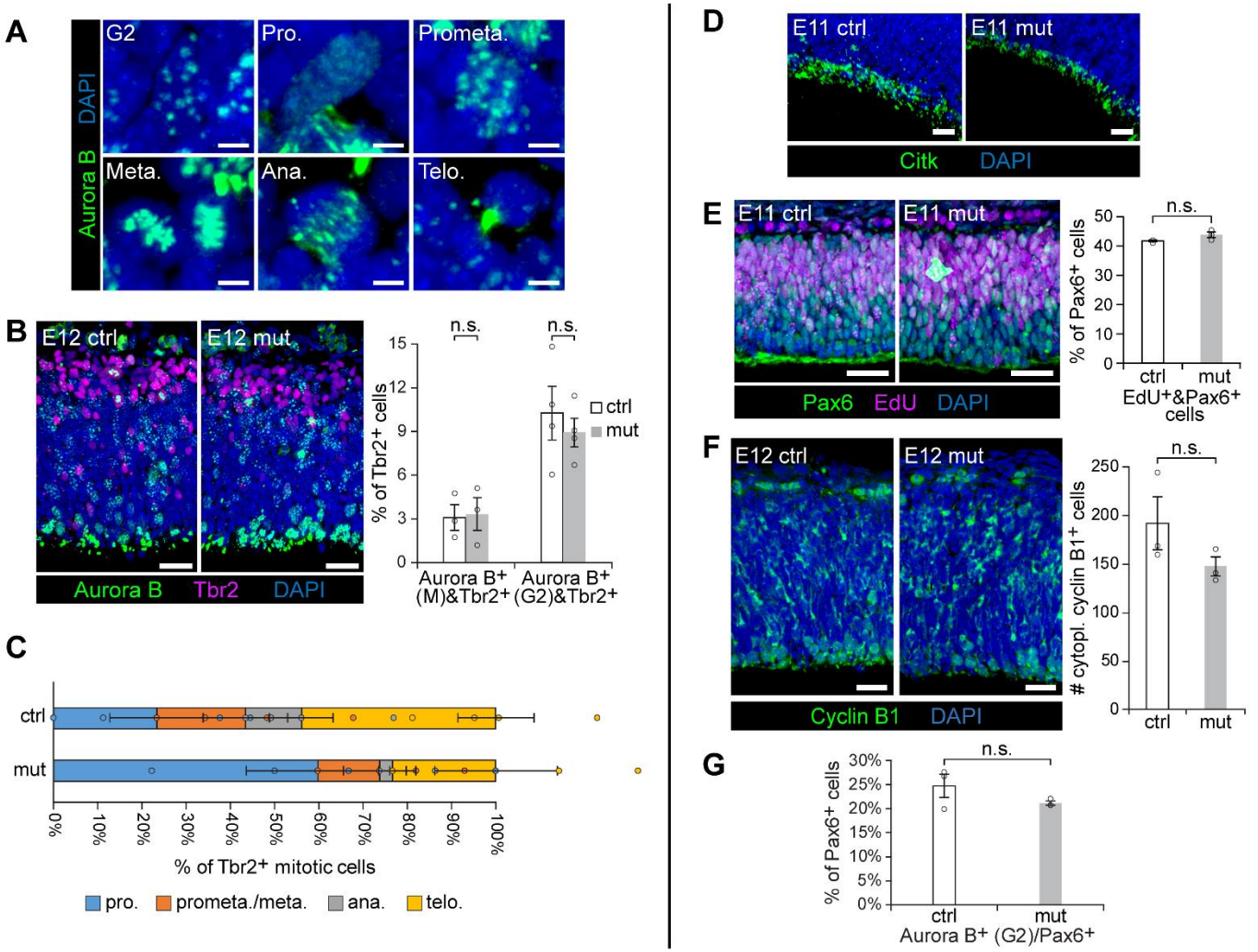

Figure S4. Cell cycle defects are not observed in the E11 mutant pallium, in IPCs of the E12 mutant pallium, or in G2 phase. Related to Figure 5. (**A**) IF for Aurora B (green, AurB) showing phase-specific Aurora B staining patterns in cells in G2, prophase (pro.), prometaphase (prometa.), metaphase (meta.), anaphase (ana.), and telophase (telo.) in the E12 pallium. Scale bars=4 µm. (**B**) IF for Aurora B (green) and Tbr2 (magenta) in sagittal sections of control (ctrl) and mutant (mut) E12 pallium, with bar graph showing the percentage of $Tbr2^+$ cells with mitosis- and G2-specific (*N*=4) Aurora B staining patterns. (**C**) Bar graph showing the percentage of Aurora $B^+/Tbr2^+$ mitotic cells in prophase, prometaphase/metaphase (prometa./meta.), anaphase, and telophase (*N*=4). (**D**) IF for Citk (green) in sagittal sections of E11 control and mutant pallium. (**E**) IF for Pax6 (green) and EdU detection (magenta) in sagittal sections from E11 control (ctrl, left) and mutant (mut, right) pallium, with bar graph showing the percentage of $Pax6^+$ cells that were EdU^+ in the E11 ctrl and mut pallium. (**F**) IF for cyclin B1 (green) in sagittal sections of the E12 ctrl and mut pallium, with bar graph showing the number of cell with cytoplasmic (cytopl.) cyclin B1. (**G**) Bar graph showing the percentage of $Pax6^+$ cells with G2-specific Aurora B^+ staining in the E12 ctrl and mut pallium. Scale bars=30 µm, unless otherwise specified. Quantification data are represented as mean±SEM from *N*=3 for each condition per time-point, unless otherwise specified. Statistical significance was determined by two-tailed student's *t*-test (Table S8). n.s.=not significant.

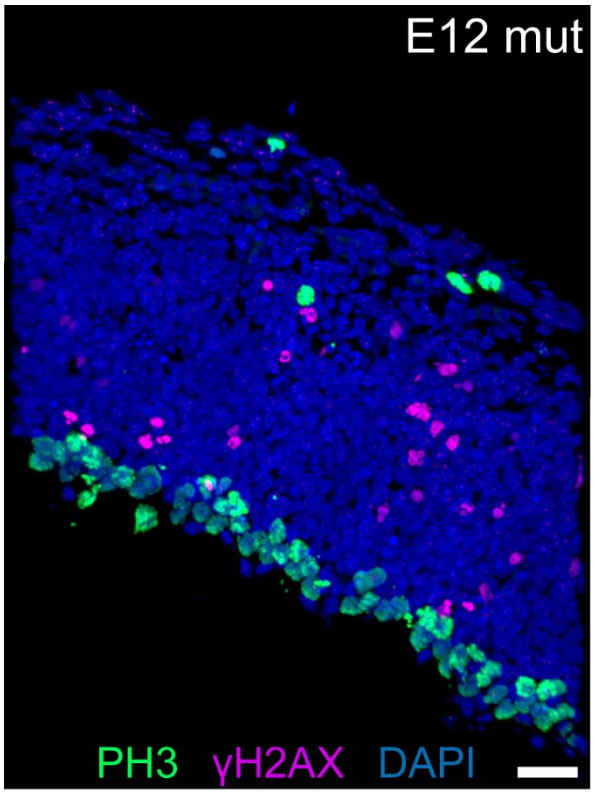

Figure S5. Cells with DNA damage are not in mitosis. Related to Figure 6. IF for PH3 (green) and γH2AX (magenta) in a sagittal section of the E12 mutant pallium. Scale bar=30 μm.

Table S1. RNAseq gene expression data. Related to Figure 4. FC=expression fold-change between control and mutant.

Click here to Download Table S1

Table S2. Mammalian functions of the 4 genes upregulated in the mutant pallium that enriched for "intrinsic apoptotic signaling pathway in response to DNA damage by p53 mediator" by DAVID. Related to Figure 4. FC=expression fold-change between control and mutant. Ave=average.

Gene	Synonyms	Ave FPKM Ctrl	Ave FPKM Mut	FC	Function Description
Bbc3	*Puma, Jfy1, Jfy-1*	0.7199858	1.8057943	2.43627	p53 upregulated modulator of apoptosis, a BH3 domain-containing gene (PMID: 11572983); alongside Pmaip1 (below), important activator of genotoxic stress-induced apoptosis in NPCs (PMID: 16822983); required for apoptosis driven by increased p53 expression (PMID: 12574499)
Eda2r	*Xedar*	1.6703153	10.5807371	6.85729	both *EDA2R* and its ligand, *EDA*, are transcriptionally activated by p53 (PMID: 19543321, 20501644); regulator of p53-mediated apoptosis via interaction with the death receptor FAS, and increased expression of EDA2R results in upregulation/stabilization of FAS protein levels (PMID: 19543321)
Perp	*Kcp1, Krtcap1, Pigpc1, Thw*	0.4671268	1.0282991	2.23922	p53 apoptosis factor related to PMP-22; transcriptionally activated by p53 during p53-mediated apoptosis, but not during p53-mediated G1 arrest (PMID: 10733530, 14707288); induces p53 upregulation, post-translational p53 modifications that disrupt MDM2-p53 binding, and p53 nuclear translocation (PMID: 21451571); important positive regulator of p53-mediated apoptosis in the embryonic mouse brain (PMID: 14614825); DNA damage upregulates *Perp* expression (PMID: 14614825)
Pmaip1	*Noxa, Apr*	0.7210288	2.3228602	2.56006	pro-apoptotic, BH3 domain-containing gene whose transcription is activated by p53 (PMID: 10807576, 14500851); alongside Bbc3 (above), important activator of genotoxic stress-induced apoptosis in NPCs (PMID: 16822983)

Table S3. Minor intron retention data, derived from RNAseq data. Related to Figure 5. *P*-values were determined by two-tailed student's *t*-test. Rep=replicate; Avg=average. MSI=mis-splicing index.

Click here to Download Table S3

Table S4. Prediction of the effect of minor intron retention in the isoforms of MIGs with significant elevation of minor intron retention in the E12 mutant pallium. Related to Figure 5. ORF=open reading frame; NMD=nonsense-mediated decay.

Click here to Download Table S4

Table S5. Mammalian functions of the 21 MIGs regulating cell cycle with significantly elevated minor intron retention the mutant pallium. Related to Figures 5, S3, and S4. *P*-values were determined by two-tailed student's *t*-test. Syns=synonyms, ave=average. MSI=mis-splicing index.

Click here to Download Table S5

Table S6. The DNA damage response functions of 14 MIGs with significantly elevated minor intron retention in the mutant pallium. Related to Figure 4. MSI=mis-splicing index. *P*-values were determined by two-tailed student's *t*-test. Syns=synonyms, ave=average.

MIG	Syns	Ave FPKM Ctrl	Ave FPKM Mut	Ave MSI Ctrl	Ave MSI Mut	MSI *P*-value	ΔMSI	DNA Damage Response Function Description
Baz1b	*Wstf, Wbscr9, Wbscr10*	21.907384	25.945518	5.447441	12.41971	0.019728	13.97227	forms nucleosome remodeling complex with ISWI (complex: WICH), which phosphorylates and maintains this phosphorylation of H2AX (ɣH2AX), thereby regulating important steps in the DNA damage response process (PMID: 19092802)
Ccnk	*Cpr4, CycK*	55.348807	5.326979	5.053107	27.09289	0.004641	22.03978	cyclin K; when complexed with Cdk9, accumulates on chromatin in response to replication stress, and ssDNA in stressed cells (PMID: 20930849)
Cep164	*Nphp15*	5.060874	5.324126	5.904086	30.06079	0.000429	24.156701	centrosomal protein that is phosphorylated by the DNA damage response proteins ATR and ATM; siRNA-mediated knockdown in HeLa cells results in reduced phosphorylation of multiple DNA damage response proteins and chromosome missegregation (PMID: 18283122)
Cul1		41.697261	47.309440	2.804814	16.18051	0.001812	13.3757	as part of the SCF E3 ubiquitin ligase complex, ubiquitinates Ku80, a component of the initiating complex of the NHEJ double-strand break DNA repair pathway, thereby regulating this complex's removal from DNA (PMID: 23324393)
Cul4a		11.101313	12.071160	3.608965	15.74483	0.044297	12.13587	cullin; ubiquitin ligase that targets Ddb1 (another MIG, below) and Ddb2, both of which act to initiate the DNA damage response, for ubiquitination and degradation, thereby regulating the DNA damage response (PMID: 19481525)
Dna2	*Dna2l*	3.9216094	3.7578457	4.807850	17.42876	0.015044	12.62091	due to 5' to 3' endonuclease activity, involved in resection extension in homologous recombination-mediated DNA double stranded break repair (PMID: 28718810)

Ddb1	*XPE, DDBA, XAP1, XPCE*	86.093717	88.333331	0.461818	2.706198	0.004385	2.244381	large subunit of DNA damage-binding complex, which functions in nucleotide excision repair (PMID: 16951172); loss of *Ddb1* in mouse brain results in accumulation of cell cycle regulators and increased genomic instability, ultimately causing apoptosis of proliferating neuronal progenitors (PMID: 17129780)
E2f1	*Rbp3, Rbap1, Rbbp3*	6.067779	6.486815	12.91249	53.23981	0.000964	40.32732	upregulated in response to DNA damage, and promotes DNA damage-induced apoptosis (PMID: 11459832); indirectly regulates the transcription of the DNA damage response gene *GADD45A* (PMID: 20713352)
Ercc5	*Xpg*	5.363914	6.275879	1.333767	7.642992	0.048076	6.309225	single strand-specific DNA endonuclease involved in the 3' incision step of nucleotide excision repair (PMID: 7657672)
Exo1	*Msa, Hex1*	4.4268470	4.1420745	3.731127	9.386061	0.008405	5.654934	5’ to 3’ endonuclease involved in DNA mismatch repair and resection extension in homologous recombination-mediated DNA double stranded break repair (PMID: 24705021)
Ints7		8.821004	8.814813	3.590800	13.52046	0.012655	9.929663	recruited to sites of DNA damage and interacts with SSB1, a DNA damage sensor recognized by ATM (PMID: 21659603)
Parp1	*Parp, Ppol, Adprt, Artd1, Adprt1*	47.879274	47.679811	0.771961	14.72329	0.002560	13.95133	nuclear protein that promotes formation of poly(ADP-ribose) chains (PARylation), which transfers ADP-ribose group from NAD+ to target protein and forms a scaffold around DNA breaks, allowing for recruitment of essential DNA damage response factors (PMID: 21989215, 22431722)
Usp10	*UBPO, Uchrp*	10.625277	8.050707	4.474797	17.26511	0.012563	12.79031	after DNA damage, phosphorylated by ATM, resulting in Usp10 stabilization and transport to the nucleus, where it deubiquitylates p53, thereby stabilizing p53 (PMID: 20096447)

Table S7. Primer sequences for RT-PCR.

Primer Name	Primer Direction	Sequence (5' to 3')
Rnu11 cKO, 5' loxP	Forward (primer 1)	ACCCTCCCCTACTGTTTTAC
	Reverse (primer 2)	AGGCTGCTACAGGATGACTC
Rnu11 cKO, 3' loxP	Forward (primer 3)	CATGTGTTTGCTGGGAATTG
	Reverse (primer 4)	CTCATGAGGCAGATCTCTGAA
Hist1h1a expression	Forward	AGAAGAACAACAGCCGCATCAAACTGG
	Reverse	CTTGGACTCAGCCTTCTTGTTCAGCTT
Cre genotyping	Forward	TATCCAGCAACATTTGGGCCAGCT
	Reverse	AACATTCTCCCACCGTCAGTACGTGA
Emx1-Cre zygosity, wild-type	Forward	AAGGTGTGGTTCCAGAATCG
	Reverse	CTCTCCACCAGAAGGCTGAG
Emx1-Cre zygosity, mutant	Forward	GATCTCCGGTATTGAAACTCCAGC
	Reverse	GCTAAACATGCTTCATCGTCGG
U11 expression	Forward	AAAGGGCTTCTGTCGTGAGTGGC
	Reverse	CCGGGACCAACGATCACCAG
Neat1 expression	Forward	AATTGGCCAGAAGACAACAGGGTTTGC
	Reverse	GTATTCAGTGGCAAAGCACTCATGAGG
Coa3 minor intron splicing	Forward	CAGTTGCAGTTTATGCGGCAGGTG
	Reverse (intronic)	CTAGCCACCCTTGCTGTTTTCCCAAA
	Reverse (exonic)	CAGCTTTGGCTTCATCTTCCAGCTC
Pten minor intron splicing	Forward	CTCCCAGACATGACAGCCATCATCAA
	Reverse (intronic)	CTACTCCCACGTTATCAGAGTGACAGAA
	Reverse (exonic)	CAAGTCTTTCTGCAGGAAATCCCATAGC
Parp1 minor intron splicing	Forward	AAAACCACCCCTGACCCTTCG
	Reverse (intronic)	GCACACAGCATAGCCAAGAAAGG
	Reverse (exonic)	AATGTACCTGGGGAGGGCAGTT
Sfrs10 expression	Forward	AGCAGGTCTTACAGCCGAGATTATCG
	Reverse	CCAAACACGCCAAGACAACAGTTG
Spc24 expression	Forward	CTCATACCTTGCACAGAACTGGGGTT
	Reverse	AATAAAAAAGAAGCTGCAGGCCAGCC
Intergenic primers	Forward	GGATAGTTCATCTCCTGCAGGTCACAAG
	Reverse	GTCCCACCCATCTAGTTTAGCATCAGC

Table S8. Summary of statistical analyses performed.

Fig.	Experimental Paradigm (ex: immuno-staining)	*N*-value	*P*-value	t/f-value	Statistical test	Test for multiple testing?	Does data meet assumption of normality?
1B	qPCR	WT=3 WT/KO=3	6.43E-05	17.38388	Student's t-test [1]	No	Yes
1C	Genotype frequency	WT=20 Het=45 Mut=0	0.0001067	N/A	Chi-squared goodness of fit test	No	Yes
1J	Pallium thickness	Ctrl=3 Mut=3	0.63251 (E12) 0.96958 (E13) 0.02533 (E14)	-0.5168 (E12) 0.0405 (E13) 3.4805 (E14)	Student's t-test [1]	No	Yes

2A	TUNEL	Ctrl=3 Mut=3	0.587853	-0.58845	Student's t-test [1]	No	Yes
2B	TUNEL	Ctrl=4 Mut=4	0.000364	-7.19759	Student's t-test [1]	No	Yes
2C	TUNEL	Ctrl=3 Mut=3	0.001647	-7.55204	Student's t-test [1]	No	Yes
2D	TUNEL	Ctrl=4 Mut=4	0.017318	-3.25681	Student's t-test [1]	No	Yes
2E	CC3	Ctrl=3 Mut=3	0.348641	-1.06066	Student's t-test [1]	No	Yes
2F	CC3	Ctrl=4 Mut=4	0.006263	-4.11334	Student's t-test [1]	No	Yes
3D	Ki67	Ctrl=3 Mut=3	0.94384 (E12) 0.00114 (E13) 9.86E-05 (E14)	0.07497 (E12) 8.31546 (E13) 15.6004 (E14)	Student's t-test [1]	No	Yes
3D	NeuN	Ctrl=3 Mut=3	0.58591 (E12) 0.50374 (E13) 0.00256 (E14)	0.59165(E12) 0.73383 (E13) 6.71922 (E14)	Student's t-test [1]	No	Yes
3H	Pax6	Ctrl=3 Mut=3	0.91943 (E12) 0.00063 (E13) 2.83E-06 (E14)	0.1076 (E12) 9.6834 (E13) 38.116 (E14)	Student's t-test [1]	No	Yes
3L	Tbr2	Ctrl=3 Mut=3	0.983274 (E12) 0.030437 (E13) 0.001203 (E14)	-0.0223 (E12) 3.2822 (E13) 8.2035 (E14)	Student's t-test [1]	No	Yes
4B	qRT-PCR	Ctrl=4 Mut=4	0.000109	8.944523	Student's t-test [1]	No	Yes
4C	qRT-PCR	Ctrl=4 Mut=4	0.004161	4.487097	Student's t-test [1]	No	Yes
4E	yH2AX	Ctrl=3 Mut=3 (E11) Ctrl=3 Mut=4 (E12)	0.039021 (E11) 0.027471 (E12)	-3.02372 (E11) -4.02969 (E12)	Student's t-test [1] (E11) T-test: two sample assuming unequal variances (E12)	No	Yes
4E	P53	Ctrl=3 Mut=3 (E11) Ctrl=3 Mut=4 (E12)	0.57902 (E11) 0.01497 (E12)	0.60302 (E11) -5.05123 (E12)	Student's t-test [1] (E11) T-test: two sample assuming unequal variances (E12)	No	Yes
4G	Pax6/ p53	Mut=3	P<0.001 (Fisher's method) 0.1651 (N=1) 2.53E-04	N/A	Fisher Exact test[2]	No	Yes

			(N=2) 6.72E-04 (N=3)				
5C	Ki67/ PH3	Ctrl=5 Mut=5	0.036877	-2.50113	Student's t-test [1]	No	Yes
5D	Pax6/ AuroraB (M)	Ctrl=3 Mut=3	0.281507	-1.24374	Student's t-test [1]	No	Yes
5E	Pax6/ AuroraB	Ctrl=4 Mut=4	0.050205 (prophase) 0.022396 (prometaphase/ metaphase) 0.399731 (anaphase) 0.853745 (telophase)	2.443901 (prophase) -3.05402 (prometaphase/ metaphase) 0.906253 (anaphase) 0.19244 (telophase)	Student's t-test [1]	No	Yes
5F	Citk	Ctrl=3 Mut=3 (E11) Ctrl=4 Mut=4 (E12)	0.909922 (E11) 0.001502 (E12)	-0.1205 (E11) 5.5091 (E12)	Student's t-test [1]	No	Yes
5G	Pax6/ EdU	Ctrl=3 Mut=4	0.00013	10.58504	T-test: two sample assuming unequal variances	No	Yes
5H	Tbr2/ EdU	Ctrl=3 Mut=3	0.143103	1.972462	Student's t-test [1]	No	Yes
6A	yH2AX/ EdU	Mut=3	0.5<P<0.6 (Fisher's method) 0.0953 (n=1) 0.762 (n=2) 1.0 (n=3)	N/A	Fisher Exact test[2]	No	Yes
6B	P53/EdU	Mut=3	P<0.001 (Fisher's method) 0.0095 (N=1) 0.4087 (N=2) 4.61E-06 (N=3)	N/A	Fisher Exact test[2]	No	Yes
6C	P53/ AuroraB (M)	Mut=4	P<0.001 (Fisher's method) 3.94E-06 (N=1) 3.24E-04 (N=2) 0.0135 (N=3) 0.0115 (N=4)	N/A	Fisher Exact test[2]	No	Yes
6C	P53/ AuroraB (G2)	Mut=4	P<0.001 (Fisher's method) 9.18E-05	N/A	Fisher Exact test[2]	No	Yes

			(N=1) 2.76E-06 (N=2) 0.0321 (N=3) 2.01E-07 (N=4)				
6D	EdU/CC3	Mut=3	0.4<P<0.5 (Fisher's method) 0.345 (N=1) 0.586 (N=2) 0.265 (N=3)	N/A	Fisher Exact test[2]	No	Yes
S2C	CC3/pyknotic cells	Ctrl=3 Mut=3	0.001891	-7.28116	Student's t-test [1]	No	Yes
S2C	CC3/Tuj1	Ctrl=3 Mut=3	0.140357	-1.83533	Student's t-test [1]	No	Yes
S2D	Pax6	E12=3 E13=3 E14=3	0.001 (ANOVA) 0.002 (E12-E13) 0.719py (E13-E14)	30.835 (ANOVA)	One–way ANOVA	Post-hoc Tukey	Yes
S2E	Tbr2	E12=3 E13=3 E14=3	0.046 (ANOVA) 0.284 (E12-E13) 0.039 (E13-E14)	5.351 (ANOVA)	One–way ANOVA	Post-hoc Tukey	Yes
S2F	BrdU/ NeuN	Ctrl=3 Mut=3	0.0115 (%NeuN) 0.96281 (%BrdU)	4.416383 (%NeuN) 0.049606 (%BrdU)	Student's t-test [1]	No	Yes
S3A	qRT-PCR	Ctrl=3 Mut=3	0.009763 (Coa3) 0.014807 (Pten) 2.13E-06 (Parp1)	-4.6360 (Coa3) -4.1038 (Pten) -40.90389 (Parp1)	Student's t-test [1]	No	Yes
S4B	Tbr2/ AuroraB	Ctrl=4 Mut=4 (G2) Ctrl=3 Mut=3 (M)	0.544268 (G2) 0.890293 (M)	0.642447 (G2) -0.14693 (M)	Student's t-test [1]	No	Yes
S4C	Tbr2/ AuroraB	Ctrl=4 Mut=4	0.109109 (prophase) 0.640059 (prometaphase/ metaphase) 0.266296 (anaphase) 0.258209 (telophase)	-1.8803 (prophase) 0.492213 (prometaphase/ metaphase) 1.225527 (anaphase) 1.248928 (telophase)	Student's t-test [1]	No	Yes
S4E	Pax6/ EdU	Ctrl=3 Mut=3	0.114046	-2.01577	Student's t-test [1]	No	Yes
S4F	Cyclin B1	Ctrl=3	0.196738	1.547139	Student's	No	Yes

		Mut=3			t-test [1]		
S4G	Pax6/ AuroraB (G2)	Ctrl=3 Mut=3	0.223782	1.438129	Student's t-test [1]	No	Yes

[1] Two-sample t-test assuming equal variances
[2] Followed by Fisher's method to combine *P*-values